Characterization of Polarization-Maintaining Fiber Using High-Sensitivity Optical-Frequency-Domain...

Article *in* Journal of Lightwave Technology · December 2006

DOI: 10.1109/JLT.2006.883607 · Source: IEEE Xplore

CITATIONS
29

READS
76

5 authors, including:

Mark Froggatt
Intuitive Surgical
82 PUBLICATIONS **1,111** CITATIONS
SEE PROFILE

Stephen T. Kreger
Luna Innovations, Inc.
42 PUBLICATIONS **301** CITATIONS
SEE PROFILE

Brian J. Soller
Luna Innovations, Inc.
37 PUBLICATIONS **612** CITATIONS
SEE PROFILE

Characterization of Polarization-Maintaining Fiber Using High-Sensitivity Optical-Frequency-Domain Reflectometry

Mark E. Froggatt, Dawn K. Gifford, Steven Kreger, Matthew Wolfe, and Brian J. Soller

***Abstract*—Optical-frequency-domain reflectometry is used to measure the group-index difference and the refractive-index difference (i.e., beat length) between the fast and slow modes in polarization-maintaining optical fiber. The Rayleigh scatter normally present in the fiber is measured in reflection. This measurement, in turn, enables a distributed measurement of the fiber's birefringence that is rapid and completely nondestructive.**

***Index Terms*—Birefringence, fiber characterization, optical-frequency-domain reflectometry (OFDR), polarization-maintaining (PM) fiber.**

I. Introduction

POLARIZATION-MAINTAINING (PM) fiber is a widely deployed and critical part of fiber-optic communications equipment. As a result, understanding the effects of PM fiber in optical systems is a relevant and not always straightforward issue. For example, the birefringence of PM fiber, which is its most distinguishing feature, can be a particularly difficult parameter to measure.

Several methods for measuring fiber birefringence have been developed over the years as fiber-measurement technology has advanced. Many initial fiber-birefringence characterization protocols were destructive (i.e., the cutback method [1]) or required manipulation of the test fiber (i.e., the fiber-twist method [2] and the scanning lateral-force method [3]). Later characterization methods tended to rely on modulation of the optical phase or wavelength of the source [4]–[7] and operated in transmission, which measures the group-index difference and not the refractive-index difference. Low coherence interferometric techniques resulted in improved sensitivity [8], [9].

The practicality of birefringence characterization systems was greatly advanced by the development of the polarization-sensitive optical time-domain reflectometer (OTDR) [10], [11], which allowed spatially distributed measurements in reflection with up to 0.5-m resolution and tens of kilometer range. However, the spatial-resolution limit did not permit testing of short lengths of fiber (a few meters) or fiber with short beat length (a few millimeters), as in PM fiber. More recent use of polarization-sensitive optical-frequency-domain reflectometry (OFDR), first developed for fiber component testing [12], achieves the resolution required for the rapid characterization of shorter fiber lengths [13], [14]. However, as we will show analytically and experimentally, the techniques employed in [13] and [14] to measure beat length are not sufficient to measure the short beat lengths encountered in PM fiber no matter how fine the resolution.

In this paper, we show how the introduction of commercially available OFDR systems with submillimeter resolution [15]–[17] and the use of autocorrelations in the spectral domain provide a new and more easily implemented method of characterizing fiber birefringence. High-sensitivity high-resolution OFDR enables a polarization-diverse complex distributed measurement of the Rayleigh scatter along a fiber. Here, we demonstrate that this measurement, in turn, can be used to characterize a fiber's birefringence, even when the associated beat length is on the order of millimeters, and the beat patterns observed in earlier publications [13], [14] are no longer visible.

Whereas previous methods based on high-resolution OFDR have employed a Fourier-transform technique to calculate beat length [13], [14] from the time-domain amplitude data, the method described in this paper employs a distributed autocorrelation of the spectrum of the scatter pattern from the fiber under test (FUT). Use of the distributed autocorrelation of the Rayleigh spectral signature of the FUT to calculate phase birefringence and the Rayleigh temporal signature to calculate group birefringence enables the full high-resolution potential of the OFDR technique and forms the basis for the results presented in the following sections.

This method provides several advantages not previously available. First, the OFDR-based measurements presented here require no special preparation of the fiber or network and can be conducted on fiber already "pigtailed" to a device. If the fiber has a connector, the total measurement time, including all preparation and setup of the apparatus, is less than 20 s. Second, the high-spatial resolution of this technique enables measurement of short fiber lengths (a few meters) and of PM fiber with very short beat length (a few millimeters). Finally, measurements of Rayleigh scatter using OFDR are distributed over the length of the fiber enabling identification of local fluctuations in the fiber backscattering coefficient due to bends, crimps, or temperature variations. These local variations can be distinguished from the nominal birefringence characteristics of the fiber.

Characterization of the birefringence of PM fiber requires measurements of both the differential group delay (DGD) and

Manuscript received April 30, 2006; revised July 21, 2006.

The authors are with the Luna Technologies, Blacksburg, VA 24060 USA (e-mail: froggattm@lunatechnologies.com).

Digital Object Identifier 10.1109/JLT.2006.883607

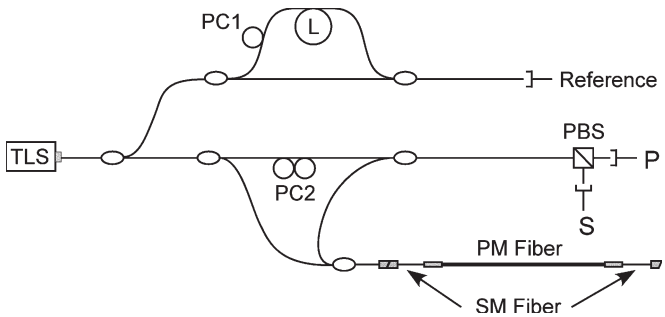

Fig. 1. Diagram of measurement setup showing the tunable laser source, the reference interferometer with Polarization Controller 1 (PC1) to prevent fringe fading, and a delay length L, which determines the sampling increment on detectors S and P. Polarization Controller 2 (PC2) is used to ensure that the reference power is split equally at the PBS between the S and P modes. The sample fiber is a segment of PM fiber with connectorized SM fiber segments spliced on the ends.

beat length. DGD is defined as the difference in propagation time between light polarized along the fast and the slow axis of the fiber. Beat length is defined as the distance over which light propagating along the fast and slow axis realizes a 2π phase shift. In order to relate DGD to beat length, we think of beat length as a phase effect, and we associate with it a phase delay. Soon, after the manufacture of PM fiber became routine, it was noted that the DGD and the phase delay (i.e., beat length) in strongly birefringent fibers do not always correspond, and that the DGD could exceed the phase delay by up to a factor of three [18], [19]. Recent work confirms that modern fiber designs continue to exhibit this property [20], especially in fibers with large form-induced birefringence.

As stated above, the techniques described here rely on distributed measurement of the complex Raleigh-scatter pattern of the FUT. The results are based upon the fundamental assumption that the Rayleigh scattering of both of the polarization modes of the FUT, whether those modes are degenerate (SMF) or not (PM), results from the same underlying pattern of defects. As a result, changes in the refractive-index scale the Raleigh-scatter pattern in frequency whereas changes in the group velocity scale the scatter pattern in delay. The scaling in frequency provides the same phenomenon as the splitting of Bragg-grating spectra that are written into PM fiber. The scaling of delay is the same phenomenon that causes DGD. The OFDR method provides the unique ability to characterize the full complex response of an optical system enabling the analysis of both time-domain and frequency-domain data in a single instrument and a single measurement. Time-domain analysis yields a measurement of the delay scaling, or DGD, where frequency-domain analysis provides a measure of the frequency scaling or the change in refractive index.

II. Measurement SetUp

The OFDR instrument has been described in earlier publications [15]–[17] but is reproduced here for clarity. Fig. 1 shows a diagram of the measurement network. The system operates by sweeping a tunable laser over a range of wavelengths. In the case of PM fiber measurement, a wide sweep range (1530 to 1570 nm) is used to produce high-resolution (20 μm) spatial data. Since the polarization state of the returning signal is arbitrary, we must employ a polarization diverse detection scheme. In this case, a polarization controller PC2 is used to adjust the polarization of the light in the reference path of the measurement interferometer (lower interferometer) such that it is split evenly between the two states of the polarization beam splitter (PBS). The interference fringes are then digitized as a function of laser frequency and stored in memory. The reference interferometer (upper interferometer) provides a high-resolution measurement of the laser tuning required for obtaining high-resolution transform data. A Fast Fourier Transform (FFT) then converts this frequency-domain data into time-domain data. Since two channels of data were recorded (one for each polarization), all of the optical power reflected from the DUT has been detected, and, when properly scaled, the powers at each point can be summed to give the total power reflected from that particular delay.

If the dynamic range and sensitivity are sufficient, OFDR systems like this can be used to detect the scatter off of the optical fiber core, with a signal to noise ratio as high as 17 dB. The scatter profile from a segment of optical fiber is comprised of a random set of complex numbers and represents a permanent structure in the fiber core. It is upon this complex scattering structure in the fiber core that we construct the beat-length measurement technique.

III. Analysis of Scatter From PM Fiber

We begin by assuming a continuous but random scattering cross section $\kappa(z)$ along a section of fiber, which represents the amplitude and phase of the light reflected from the fiber as a function of distance z. Its transform $K(\eta)$ is the spatial spectrum of this segment of fiber, where η is a spatial frequency. Only one polarization mode is considered at the moment; the other will be added by superposition later. The scatter, as a function of laser frequency ω, can be expressed as

$$E(\omega) = E_0 \int_0^L \kappa(z) e^{-i2k(\omega)z} dz \tag{1}$$

where $k(w)$ represents the dispersion relation of the fiber. Since the scattering is very weak, we can assume that the incident electric field is unaffected by the scatter and can be represented by E_0. The range of the integration is arbitrary and could be over any segment of the fiber. Over the spectral range of interest (1530–1570 nm), we will assume that $k(\omega)$ is linear and given by

$$k(\omega) = \beta \frac{\omega}{c} + \gamma \tag{2}$$

where c is the speed of light in a vacuum, β is a constant group index, and γ is another constant accounting for the presence of dispersion [18]. The refractive index n_{ref} is given by

$$n_{\text{ref}}(\omega) = \beta + \gamma \frac{c}{\omega}. \tag{3}$$

Substituting for k

$$E(\omega) = E_0 \int_0^L \kappa(z) e^{-i2\left(\beta\frac{\omega}{c}+\gamma\right)z} dz. \tag{4}$$

By definition, the spectral response to the laser frequency is a scaled and shifted version of the transform spatial spectrum of the scatter pattern in the fiber segment

$$E(\omega) = E_0 k \left(2\beta\frac{\omega}{c} + 2\gamma\right). \tag{5}$$

Conversion to the time domain is accomplished using a Fourier transform of (4)

$$\frac{1}{2\pi}\int_{\infty}^{-\infty} E(\omega) e^{i\omega t} dw = \frac{E_0}{2\pi}\int_{\infty}^{-\infty}\int_0^L \kappa(z) e^{-i2\left(\beta\frac{\omega}{c}+\gamma\right)z} dz e^{i\omega t} dw. \tag{6}$$

The extension of the integral to include all frequencies positive and negative allows for analytical integration over ω. This integration yields a Dirac delta. Integrating over the Dirac delta gives

$$E(t) = E_0 \frac{c}{2\beta}\kappa\left(\frac{c}{2\beta}t\right) e^{i\gamma\frac{c}{\beta}t}. \tag{7}$$

The extension to positive and negative frequencies is a computational tool that we employ for ease of representation. The data sets are only measured over a finite bandwidth defined by the tuning range of the laser, which is in this case 1530 nm–1570 nm. When we carry out digital data manipulation, the integration is only carried out over frequencies in this bandwidth, and the associated results (beat length, birefringence, etc.) are therefore bandwidth limited. This does not present a problem as the measured quantities are typically represented with an associated bandwidth of interest.

The measured time-domain response is then a scaled version of the spatial extent of the scatter. It is this scaling group index β along with the speed of light that is used to scale the horizontal axis of plots to more familiar units of distance rather than the exact and calibrated units of time. The effects of γ show up only as a rotation rate on the phase and do not affect the amplitude plot of the scatter.

We now assemble the results into a vector field by defining the two orthogonal axes of the fiber to be the slow axis $\hat{s}$ and the fast axis $\hat{f}$

$$\vec{E}(\omega) = E_{0_s} K\left(2\beta_s\frac{\omega}{c} + 2\gamma_s\right)\hat{s} + E_{0f} K\left(2\beta_f\frac{\omega}{c} + 2\gamma_f\right)\hat{f} \tag{8}$$

and

$$\vec{E}(t) = E_{0_s}\frac{c}{2\beta_s}\kappa\left(\frac{c}{\beta_s}\frac{t}{2}\right) e^{i\gamma_s\frac{c}{\beta_s}t}\hat{s} + E_f\frac{c}{2\beta_f}\kappa\left(\frac{c}{\beta_f}\frac{t}{2}\right) e^{i\gamma_f\frac{c}{\beta_f}t}\hat{f}. \tag{9}$$

One difficulty that is immediately apparent is that when the axis is scaled to distance using a choice of group index, only one of the polarization states can read correctly. In this paper, the average group index has been used for the scaling of the horizontal axis. The differences between the group indexes are actually quite small, and the scaling effects in the spectral responses of (9) are minor, with the predominant effect being an apparent offset in addition to that caused by γ.

IV. Experimental Results

As shown in Fig. 1, the FUT was a segment of PM fiber, Fibercore HB1250P, with standard SM fiber spliced to both ends. Each end of this spliced segment was terminated with an FC/APC connector. Fig. 2 shows the reflected amplitude as a function of distance down the fiber as found by using an FFT to transform the measured frequency-domain information into the time domain and scaling the time axis to distance, as discussed above. Reflections at the splice points are evident as peaks at about 0.5 and 3 m, as is the higher scatter level in the PM fiber between these two points. The scatter level of the SM fiber is 3.5 dB lower on the output fiber (at 3 m) than it is on the input fiber, indicating a 0.9-dB one-way splice loss when splicing SMF-28 to this PM fiber. The scatter level for the PM fiber is 1.9 dB above the scatter level for the SM fiber, but if the splice loss is taken into account, we find that the scatter in this PM fiber is about 3.7 dB above that of SMF-28.

The PM fiber segment is 2465-mm long. As the splices to the PM fiber segment provide discrete reflections, the delays for the two polarization modes of the fiber can be measured precisely. The plot in Fig. 3 shows the two reflections at the far end of the fiber. Measuring the time difference between the single reflection at the "close" splice and the "far" reflections shown in Fig. 3 gives delays of 24.198 and 24.208 ns. This measurement agrees well with DGD measurements made on the fiber assembly using a commercial instrument of 5.27-ps one way. Using these measurements, the group indexes were found to be 1.4715 and 1.4721 for the two polarization modes.

If a coil of standard single-mode fiber is measured using a high-sensitivity OFDR instrument, the induced birefringence can be clearly seen as a periodic exchange in the power between the two detected polarization states [14], [15]. If the states of the PBS happened to match the principle states of the coil, no beating would be visible. However, such coincidences are rare, and the periodic exchange of power as the light travels down the fiber is generally visible whenever a coil is measured.

Since the effects of mild birefringence are readily observable, one might expect the rotation of the polarization state in PM fiber to be particularly pronounced. With a beat length of a millimeter or more and a spatial resolution of 20 μm, such beats should be readily observed. In practice, however, such patterns are only observable in the first few centimeters of the PM fiber and then gradually fade away. The inset plot of Fig. 2 is an example of this fading of the beat fringes. As a result, direct observation of the beat frequency does not provide an accurate measurement of the beat length of PM fiber over its entire length.

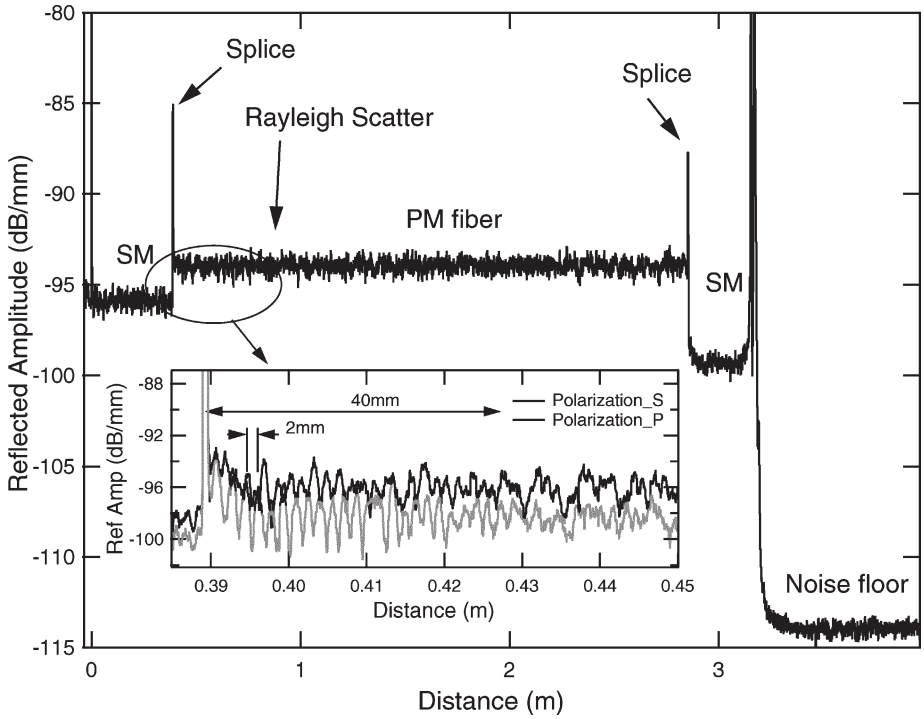

Fig. 2. Scatter amplitude versus distance measurement of the PM fiber. Inset high-resolution plot of the scatter returned in the two detected polarization states. Over the first few centimeters, the beating between the polarization states is visible.

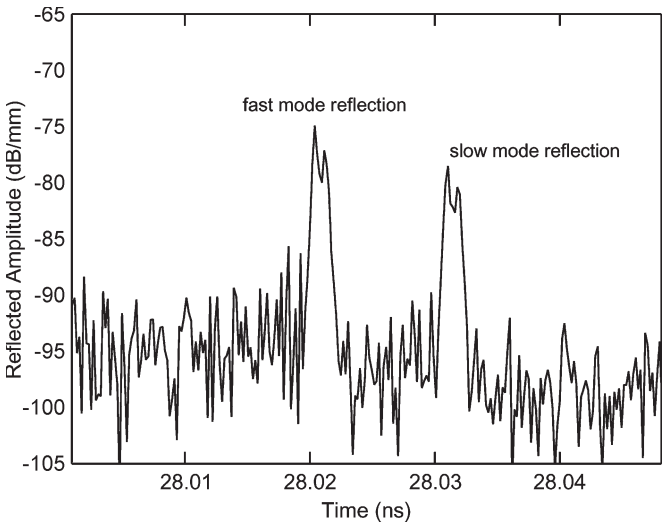

Fig. 3. Scatter amplitude versus distance measurement of the end of the PM fiber. This high-resolution plot of the fiber response is shown without scaling of time to distance. Using the time measured between the close splice reflection and the far splice reflections, the group index can be found and subsequently used to plot scatter against distance instead of time.

This fading of the beat fringes can be understood as a decorrelation of the Rayleigh-scatter patterns. As the two modes of the PM fiber propagate down the fiber, the fast mode gets ahead of the slow mode. Once the spatial difference between the two modes exceeds the spatial resolution of the instrument, the reflected light having the same delay—and thus summed at the instrument—comes from two entirely different segments of the fiber with uncorrelated phases. As a result, the relative phase between the two polarization states is entirely random, and the beat-length signature is lost. As mentioned above, using a commercial instrument, the fiber was measured to have a DGD of 5.27 ps in transmission. Assuming a constant DGD along the fiber, the rate of dispersion is 2.14 ps/m. Since the resolution of the OFDR is about 20 μm and the system is double-pass (operating in reflection), the decoherence length is expected to be 47 mm. This seems to agree well with the data shown in the left inset plot of Fig. 2, where the beating between the two modes appears to fade after about this distance.

The information needed to find the local beat length of the fiber is not lost as a result of this beat pattern fading. Since the scatter pattern is the superposition of the scatter from the two polarization modes, when the autocorrelation of the time-domain scatter pattern is calculated, a side peak shows up at the average delay difference between the two modes. The further into the fiber the segment is taken from, the larger the observed time shift, until at the end of the PM fiber segment, the time shift will be equal to the observed DGD of the fiber segment. Fig. 4 is a plot of this time shift along the length of the PM fiber. Note that the time shift is still apparent, although flat, in the SM fiber on the far side of the PM fiber. There is an effective double image of the SM fiber that occurs as a result of being observed through the PM fiber. This autocorrelation technique, therefore, provides a distributed measurement of DGD in the fiber. A numerical derivative of the curve in Fig. 4 will give the value, in units of [ps/m], of this birefringence.

A similar calculation can be made in the frequency domain by first transforming the complex data arrays associated with the fiber segment back into the frequency domain and then forming the amplitude array as a function of optical frequency. Once again, the responses of both polarization modes are

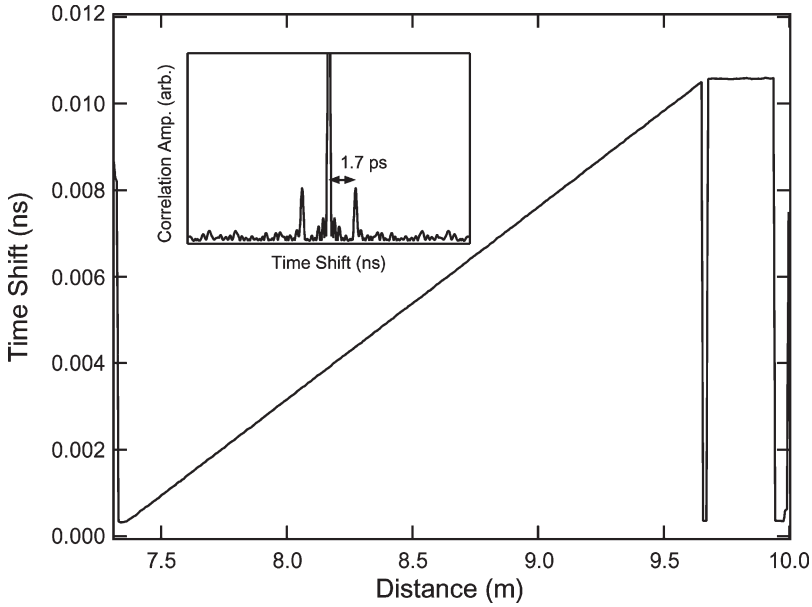

Fig. 4. Plot of the time shift to the side peak, as shown in the inset along the length of the fiber. The short drop to near zero around 9.7 m is the result of the splice reflection causing an erroneous peak measurement. Beyond the splice, however, the segment of SM fiber shows a time-shifted peak because it is observed through the PM fiber. The single-pass time shift (half the plotted two-pass value) is 5.28 ps, and the DGD measured in transmission using an optical vector analyzer was 5.27 ps.

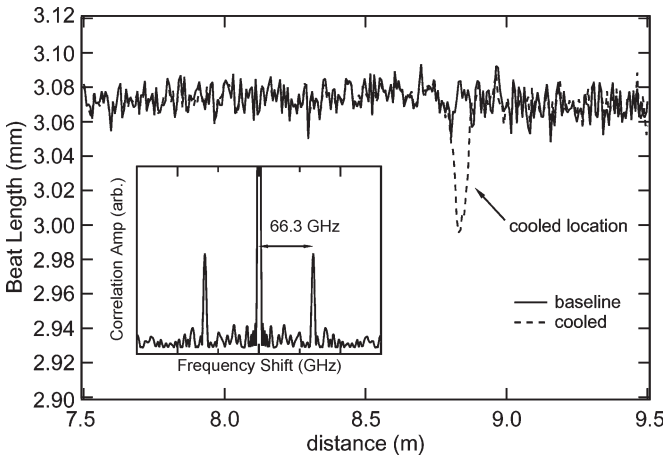

Fig. 5. Spatial variation of the beat length of the PM fiber as calculated from the frequency shift of the autocorrelation function as shown in the inset graph. Two measurements of the fiber were made; in the second measurement, a piece of ice was placed on the fiber to induce local cooling, which decreased the beat length locally. Note that the variability outside the cooled segment is highly repeatable.

present in the spectrum, and an autocorrelation of the spectrum reveals two side peaks.

The spectral splitting of fiber Bragg gratings in response to fiber birefringence has been observed numerous times [21]. This shifting of the random spectra of the fiber core originates from the same effect. We can see from (5) that the index of refraction has a strong effect on the location of the autocorrelation peaks in this domain. Although the transformation of the frequency argument is actually a scaling and a shift, because the range of the scan (5 THz) compared with the average frequency (193 THz) is small, the scaling effects appear predominantly as shifts.

Fig. 5 shows the frequency shift between the zero-shift autocorrelation peak and the side autocorrelation peak as a function of distance along the PM fiber. An example autocorrelation plot is inset. As a demonstration of the distributed nature of the measurement, a short segment of the fiber was cooled using a piece of ice. The cooling further increased the stress levels in the fiber and thus increased the frequency shift. The data shown here were processed in 2-cm segments and show remarkable repeatability over the segments of fiber that were not cooled.

The autocorrelation data obtained in the frequency domain, when combined with the time-shift data from the time domain and the length measurement of the fiber, allow one to calculate the beat length of the fiber segment. We begin by recognizing that the distance to the side peaks is the frequency shift at which the field in the fast mode propagates with the same wave length as the slow mode or

$$k_f(\omega_1) = k_s(\omega_2) = k_s(\omega_1 + \Delta\omega) \tag{10}$$

where $\Delta\omega$ is the measured frequency shift in radians per second. Substituting our presumed form for the dispersion relation in (5) gives

$$k_f(\omega_1) = \beta_f \frac{\omega_1}{c} + \gamma_f = \beta_s \frac{(\omega_1 + \Delta\omega)}{c} + \gamma_s = k_s(\omega_2) \tag{11}$$

where the subscripts f and s denote the properties of the fast and slow modes, respectively. Simplifying to find $\gamma_f - \gamma_s$ gives

$$\gamma_f - \gamma_s = \beta_s \frac{\Delta\omega}{c} - \frac{\omega_1}{c}(\beta_f - \beta_s). \tag{12}$$

The beat length is then given by the difference in the propagation vectors at the same frequency

$$k_f(\omega_1) - k_s(\omega_1) = \beta_s \frac{\Delta\omega}{c} = \frac{2\pi}{l_{\text{beat}}}. \quad (13)$$

Inserting our measurements of group index and frequency shift gives

$$l_{\text{beat}} = \frac{2\pi c}{\beta_s \Delta\omega} = \frac{299\,792\,463 \text{ m/s}}{(1.472)(66.3 \times 10^9 \text{ Hz})} = 3.1 \text{ mm} \quad (14)$$

as the beat length in the fiber. If we use the group index alone to compute the beat length, we get a different value

$$l_{\text{beat, grp}} = \frac{2\pi c}{(\beta_s - \beta_f)\omega_1} = \frac{\lambda_1}{(\beta_s - \beta_f)} = \frac{1550 \text{ nm}}{(0.000641)} = 2.4 \text{ mm} \quad (15)$$

for the beat length, amounting to a 30% discrepancy between the measurements. This difference in the beat length when calculated using the group index verses using the propagation vector is consistent with the differences in DGD versus phase delay found in [18]–[20].

V. Conclusion

High-sensitivity OFDR enables fast and easy measurement of the distributed birefringence, both "group" and "phase," of PM fiber. It also provides other significant information about the fiber properties, including the splice loss to SM fiber, scatter level, average group index, and distributed temperature and strain effects. The most noteworthy aspect of this is that all of the characterizations are possible with a single connection to the OFDR system and a single 10-s measurement. No other setup is involved, making this a rapid and reliable technique, enabled by a measurement tool that has utility for a number of other applications.

References

[1] F. P. Kapron, "Birefringence in dielectric optical waveguide," *IEEE J. Quantum Electron.*, vol. QE-8, no. 2, pp. 222–225, Feb. 1972.

[2] S. Huang and Z. Lin, "Measuring the birefringence of single-mode fibers with short beat length or non-uniformity: A new method," *Appl. Opt.*, vol. 24, no. 15, pp. 2355–2361, Aug. 1985.

[3] K. Takada, J. Noda, and R. Ulrich, "Precision measurement of modal birefringence of highly birefringent fibers by periodic lateral force," *Appl. Opt.*, vol. 24, no. 24, pp. 4387–4391, Dec. 1985.

[4] K. Kikuchi and T. Okoshi, "Wavelength-sweeping technique for measuring the beat length of linearly birefringent optical fibers," *Opt. Lett.*, vol. 8, no. 2, pp. 122–123, Feb. 1983.

[5] P. Zhang and D. Irvine-Halliday, "Measurement of the beat length in high-birefringent optical fiber by way of magnetooptic modulation," *J. Lightw. Technol.*, vol. 12, no. 4, pp. 597–602, Apr. 1994.

[6] A. J. Barlow, "Optical-fiber birefringence measurement using a photoelastic modulator," *J. Lightw. Technol.*, vol. LT-3, no. 1, pp. 135–145, Jan. 1985.

[7] K. S. Chiang, "Acousto-optical modulation method for measuring the beat length of a linearly birefringent optical fiber," *Opt. Lett.*, vol. 14, no. 18, pp. 1029–1031, Sep. 1989.

[8] W. J. Bock, W. Urbanczyk, and M. Fontaine, "Characterization of highly birefringent optical fibers using interferometric techniques," *IEEE Trans. Instrum. Meas.*, vol. 46, no. 4, pp. 903–907, Aug. 1997.

[9] D. P. Davé and T. E. Milner, "Precise beat-length measurement of birefringent fibres with a dual-channel, low-coherence reflectometer," *Electron. Lett.*, vol. 37, no. 4, pp. 215–216, Feb. 2001.

[10] A. Galtarossa, L. Palmieri, A. Pizzinat, M. Schiano, and T. Tambosso, "Measurement of local beat length and differential group delay in installed single mode fibers," *J. Lightw. Technol.*, vol. 18, no. 10, pp. 1389–1394, Oct. 2000.

[11] F. Corsi, A. Galtarossa, and L. Palmieri, "Polarization mode dispersion characterization of single-mode optical fiber using backscatter technique," *J. Lightw. Technol.*, vol. 16, no. 10, pp. 1832–1843, Oct. 1998.

[12] J. P. von derWeid, R. Passy, G. Mussi, and N. Gisin, "On the characterization of optical fiber network components with optical frequency domain reflectometry," *J. Lightw. Technol.*, vol. 15, no. 7, pp. 1131–1141, Jul. 1997.

[13] M. Wegmüller, M. Legré, and N. Gisin, "Distributed beat length measurement in single-mode fibers with optical frequency domain reflectometry," *J. Lightw. Technol.*, vol. 20, no. 5, pp. 800–807, May 2002.

[14] B. Huttner, J. Reecht, N. Gisin, R. Passy, and J. P. von derWeid, "Local birefringence measurements in single-mode fibers with coherent optical frequency-domain reflectometry," *IEEE Photon. Technol. Lett.*, vol. 10, no. 10, pp. 1458–1460, Oct. 1998.

[15] B. Soller, D. Gifford, M. Wolfe, and M. Froggatt, "High resolution optical frequency domain reflectometry for characterization of components and assemblies," *Opt. Express*, vol. 13, no. 2, pp. 666–674, Jan. 24, 2005.

[16] M. Froggatt and J. Moore, "High spatial resolution distributed strain measurement in optical fiber using Rayleigh scatter," *Appl. Opt.*, vol. 37, no. 10, pp. 1735–1740, Apr. 1, 1998.

[17] B. Soller, D. Gifford, M. Wolfe, M. Froggatt, P. Wysocki, and M. Yu, "Measurement of localized heating in fiber optic components with millimeter spatial resolution," presented at the Optical Fiber Communications/Nat. Fiber Optic Engineers Conf., Anaheim, CA, Mar. 2006, Paper OFN 3.

[18] W. K. Burns and R. P. Moeller, "Measurement of polarization mode dispersion in high-birefringence fibers," *Opt. Lett.*, vol. 8, no. 3, pp. 195–197, Mar. 1983.

[19] S. C. Rashleigh, "Measurement of fiber birefringence by wavelength scanning: Effect of dispersion," *Opt. Lett.*, vol. 8, no. 6, pp. 336–338, Jun. 1983.

[20] M. Legre, M. Wegmuller, and N. Gisin, "Investigation of the ratio between phase and group birefringence in optical single-mode fibers," *J. Lightw. Technol.*, vol. 21, no. 12, pp. 3374–3378, Dec. 2003.

[21] R. B. Wagreich, W. A. Atia, H. Singh, and J. S. Sirkis, "Effects of diametric load on fibre Bragg gratings fabricated in low birefringent fibre," *Electron. Lett.*, vol. 32, no. 13, pp. 1223–1224, Jun. 1996.

Mark E. Froggatt, photograph and biography not available at time of publication.

Dawn K. Gifford, photograph and biography not available at time of publication.

Steven Kreger, photograph and biography not available at time of publication.

Matthew Wolfe, photograph and biography not available at time of publication.

Brian J. Soller, photograph and biography not available at time of publication.